SCIENCE CHINA
Earth Sciences

• RESEARCH PAPER •

January 2015 Vol.58 No.1: 138–150
doi: 10.1007/s11430-014-4943-z

Quality assessment of onboard GPS receiver and its combination with DORIS and SLR for Haiyang 2A precise orbit determination

GUO Jing[1], ZHAO QiLe[1*], GUO Xiang[1,2], LIU XiangLin[3], LIU JingNan[1,5] & ZHOU Quan[4]

[1] *GNSS Research Center, Wuhan University, Wuhan 430079, China;*
[2] *School of Geodesy and Geomatics, Wuhan University, Wuhan 430079, China;*
[3] *Fugro Intersite B.V., Leidschendam 2263HW, Netherlands;*
[4] *Test and Assessment Research Center, China Satellite Navigation Office, Beijing 100094, China;*
[5] *Collaborative Innovation Center of Earth and Space Science, Wuhan University, Wuhan 430079, China*

Received September 16, 2013; accepted April 8, 2014; published online September 18, 2014

The GPS, DORIS, and SLR instruments are installed on Haiyang 2A (HY2A) altimetry satellite for Precise Orbit Determination (POD). Among these instruments, the codeless GPS receiver is the state-of-art Chinese indigenous onboard receiver, and it is the first one successfully used for Low Earth Orbit (LEO) satellite. Firstly, the contribution assesses the performance of the receiver through an analysis of data integrity, numbers of all tracked and valid measurements as well as multipath errors. The receiver generally shows good performance and quality despite a few flaws. For example, L2 observations are often missing in low elevations, particularly during the ascent of GPS satellites, and the multipath errors of P1 show a slightly abnormal pattern. Secondly, the PCO (Phase Center Offset) and PCV (Phase Center Variation) of the antenna of the GPS receiver are determined in this contribution. A significant leap for Z-component of PCO up to −1.2 cm has been found on 10 October 2011. Thirdly, the obtained PCO and PCV maps are used for GPS only POD solutions. The post-fit residuals of ionosphere-free phase combinations reduce almost 50%, and the radial orbit differences with respect to CNES (Centre National d'Etudes Spatiales) Precise Orbit Ephemeris (POEs) improve about 13.9%. The orbits are validated using the SLR data, and the RMS of SLR Observed minus Computed (O-C) residuals reduces from 17.5 to 15.9 mm. These improvements are with respect to the orbits determined without PCO and PCV. Fourthly, six types of solutions are determined for HY2A satellite using different combinations of GPS, DORIS, and SLR data. Statistics of SLR O-C residuals and cross-comparison of orbits obtained in the contribution and the CNES POEs indicate that the radial accuracy of these orbits is at the 1.0 cm level for HY2A orbit solutions, which is much better than the scientific requirements of this mission. It is noticed that the GPS observations dominate the achievable accuracy of POD, and the combination of multiple types of observations can reduce orbit errors caused by data gaps and maintain more stable and continuous orbits.

Haiyang 2A, GPS receiver, multipath, precise orbit determination, phase center offset, phase center variations, DORIS, SLR

Citation: Guo J, Zhao Q L, Guo X, et al. 2015. Quality assessment of onboard GPS receiver and its combination with DORIS and SLR for Haiyang 2A precise orbit determination. Science China: Earth Sciences, 58: 138−150, doi: 10.1007/s11430-014-4943-z

The Haiyang 2A (HY2A) satellite, launched on 16 August 2011 and developed by China Academy of Space Technology (CAST) and National Satellite Ocean Application Service (NSOAS), is one of Chinese satellite missions for scientific investigation of ocean topography, dynamics, and environment. This satellite is in a 970 km sun-synchronous orbit with a nominal life time of 3 years, which includes two orbit phases. In the first phase, the satellite runs in a 14-day repeat orbit for two years. In the second phase, the satellite will orbit the Earth with a 168-day repeat cycle and a 5-day approximate repeat sub-cycle for a one year period (Zhang

*Corresponding author (email: zhaoql@whu.edu.cn)

et al., 2013). In order to collect information for disaster and weather forecasting, this satellite carries several scientific instruments including a microwave imager, a dual-band (Ku-band and C-band) radar altimeter (RA) used to measure the distance from satellite to sea surface, and a Ku-band radar scatterometer for measuring the sea surface wind field (Zhang et al., 2013). These instruments require satellite orbits to be determined within an accuracy of 10 cm. Therefore, three orbit-tracking systems, i.e., a GPS (Global Positioning System) receiver, a DORIS (Doppler Orbitography and Radiopositioning Integrated by Satellite) receiver, and a Laser-reflector array (LRA), are equipped for precise orbit determination (POD).

Historically, prior to HY2A, a series of altimetry missions have been launched for height-measuring concept validation or synoptically measuring ocean topography from space. Most missions are developed by either the United States (US) or Europe, or the joint efforts of both US and Europe. Table 1 summarizes primary information for several main altimetry missions. In addition, China launched two sister satellites, i.e., Haiyang 1A and 1B, for surveying ocean color, sea surface temperature and environment monitoring.

These altimetry missions provide vital information of ocean state variations. POD is a fundamental component of altimetry satellites. The accuracy of the orbits, particularly the radial, determines directly the quality of the altimetric products. In order to accomplish higher radial accuracy, the most and latest of aforementioned missions carried GPS and DORIS receiver as well as LRA. GPS-based POD for satellite altimetry began with the Topex/Poseidon (T/P) mission (Bertiger et al., 1994), which carried a demonstrated GPS receiver (Motorola Monarch) that tracked up to six GPS satellites (Fu et al., 1994). Compared with dynamic orbit determination using DORIS and SLR (Satellite Laser Ranging) data, the GPS observation density and geometric strength allow the use of strategy of reduced-dynamic orbit determination (Yunck et al., 1994). Furthermore, several remarkable improvements and refinements of force models, e.g., global static gravity field and solar radiation pressure (SRP), were undertaken in advance of the launch of T/P (Marschall et al., 1995). Other significant improvements were made for tracking systems as well. These improvements resulted in better than 4 cm accuracy in radial component in the 1990s (Tapley et al., 1994). With the latest developments in measurement models, data processing strategy and geophysical models (e.g., static and temporal gravity field, ocean tide, and pole tide), the radial accuracy of T/P orbits computed with GPS, DORIS, and SLR data is better than 2 cm (Lemonie et al., 2010), which is far better than the requirement of 13 cm radial orbit accuracy.

The BlackJack receiver developed by NASA's JPL (Jet Propulsion Laboratory) is the main receiver used for altimetry missions (e.g., Jason-1 and Jason-2). This receiver is semicodeless and is able to track up to 16 GPS satellites on two frequencies (Haines et al., 2004). Because of sensitivity to the irradiation, the BlackJack receivers frequently lose data over South Atlantic anomaly. In addition, the phase tracking on the Jason receivers is prone to have occasionally half-cycle slips. Jason-1 is equipped with the second generation DORIS receiver that has two receiving channels (the first generation has only one channel). This increases numbers of observations as it can simultaneously track two different ground beacons. However, the ultra-stable oscillator (USO) is not as stable as expected, because its frequency is

Table 1 Summary of information for several main altimetry missions

Satellite	Launch date	End date	Altitude (km)	Inclination	Repetitivity (days)	POD instruments	Altimeter	Agency
Geosat	1985-03-12	1990-01-31	800	108°	~23.07 for GM [a)] 17.05 for ERM [b)]	Doppler	RA	US Navy
ERS-1	1991-07-17	2000-03-31	785	98.52°	3, 35, 168	PRARE [c)] LRA	RA (Ku band)	ESA [d)]
ERS-2	1995-04-21	2011-07-06	785	98.52°	35	PRARE LRA	RA	ESA
GFO	1998-02-10	2008-11-26	800	108°	17	GPS DORIS LRA	RA (Ku band)	US Navy/NOAA [e)]
Topex/Poseidon	1992-08-10	2006-01-18	1336	66°	9.9156	GPS DORIS LRA	Topex (C and Ku bands)/ Peseidon (Ku band)	NASA/CNES [f)]
Jason-1	2001-12-07	2013-07-03	1336	66°	9.9156	GPS DORIS LRA	Poseidon-2 RA	NASA/CNES
Jason-2	2008-06-20	–	1336	66°	9.9151	GPS DORIS LRA	Poseidon-3 RA	NASA/NOAA/CNES/ EUMETSAT [g)]
HY2A	2011-08-15	–	971	99.3°	14, 168	GPS DORIS LRA	Chinese indigenous RA (Ku and C bands)	CAST/NSOAS

a) GM, Geodetic Mission; b) ERM, Exact Repeat Mission; c) PRARE, Precise Range and Range-Rate Equipment; d) ESA, European Space Agency; e) NOAA, National Oceanic and Atmospheric Administration; f) CNES, Centre National d'Etudes Spatiales; g) EUMETSAT, European Organization for the Exploitation of Meteorological Satellites.

sensitive to both the irradiation rate and the total irradiation encountered in orbit. To reduce the sensitivities, a model developed by Lemoine and Capdeville (2006) can be used. The new generation DGXX DORIS instruments equipped on Jason-2 and HY2A are made in a single box with two systems, each containing one receiver and one USO as well as seven processing units of dual-frequency (Auriol and Tourain, 2010). Compared to the previous ones, the new onboard DORIS instrument has the capacity to track seven ground beacons simultaneously, resulting in a significant increase in numbers of observations. The DORIS also produces phase measurements, which are similar to the phase measurements of GPS. In addition, the new USO can reduce the sensitivity to radiation by a factor of 10 (Auriol and Tourain, 2010). Other improvement is in modeling the radiation forces for Jason-1, developed by the University College London (UCL) (Ziebart, 2004). Based on the above mentioned improvements, the radial accuracy of better than 1 cm can be achieved for Jason-1 and Jason-2 (Luthcke et al., 2003; Haines et al., 2004; Bertiger et al., 2010; Lemoine et al., 2010).

However, as to China, due to the limitation of POD instruments, the orbit accuracy for previous launched LEO satellites such as Haiyang 1A and Haiyang 1B is at decimeter or meter level. HY2A is the first Chinese satellite carried an experimental Chinese indigenous onboard GPS receiver, which tracks GPS signals on two frequencies. Although some publications have demonstrated that the radial accuracy for HY2A could achieve 2–3 cm with GPS observations only (Guo et al., 2012; Guo J et al., 2013; Jiang et al., 2013), there is no publication about the performance of this receiver. The analysis of the receiver's characteristics is rather important, because it can not only help us improve the POD accuracy but also suggest how to further improve its quality. This contribution will assess the performance of HY2A onboard receiver. In addition, HY2A also carries DORIS and LRA instruments for POD. Zhao et al. (2012) determined the POD for HY2A, and 3 cm accuracy was achieved for radial component using SLR data only. Guo J Y et al. (2013) used the simulated GPS, DORIS and SLR data to demonstrate that the cm level accuracy could be achieved for HY2A POD. In this contribution, we will demonstrate the radial accuracy currently achieved for HY2A with combination of real GPS, DORIS, and SLR data.

1 General information about HY2A mission

The HY2A satellite is equipped with two 12-channel dual-frequency GPS SSTIs (Satellite-to-Satellite Tracking Instruments), each consisting of an independent receiver and antenna. The primary unit (SSTI-A) is running in nominal operations, whereas the secondary one serves as a redundant unit (SSTI-B). In addition, a DGXX DORIS instrument and an LRA developed by CNES and Wuhan University respectively are also installed on the satellite. Figure 1 shows a schematic view of the HY2A satellite with locations of the SSTI antennas, DORIS antenna, and LRA in the right-handed SRF (Satellite Reference Frame). The SRF is defined as follows: the middle points of satellite bottom is defined as the origin of the frame, the *Z*-axis opposites to the radial direction, the *X*-axis is perpendicular to the *Z*-axis in the orbit plane and points to the velocity direction, and the *Y*-axis completes the reference with pointing to the inverse cross-track direction. Currently, the satellite attitude model adopted for HY2A assumes that the satellite is flying with a fixed orientation coinciding with SRF. Because of the fuel consumption on orbit, the center of mass (CoM) is slightly moving during the lifetime of the satellite. Table 2 shows the initial coordinates of the CoM in the SRF and the variation for the period considered in this contribution (from 1 October 2011 to 31 May 2012), as well as positions of the reference points of SSTI-A antenna, DORIS 2 GHz phase center and spherical center of LRA in the SRF. In addition, a bias of 73.7 mm should be added for correcting SLR measurements from the phase center to the spherical center (Wu, 2012).

2 Performance of HY2A onboard GPS receiver and other available data

2.1 Onboard GPS receiver and data characteristics

The onboard GPS receiver of HY2A is developed by Space Star Technology Co., Ltd. and is the state-of-art Chinese indigenous onboard GPS receiver. This receiver uses the codeless tracking technique and has been specifically designed for orbital application. It supports two antenna inputs, which are individually assigned to any of the 12 tracking channels. Our previous analysis based on the zero baseline

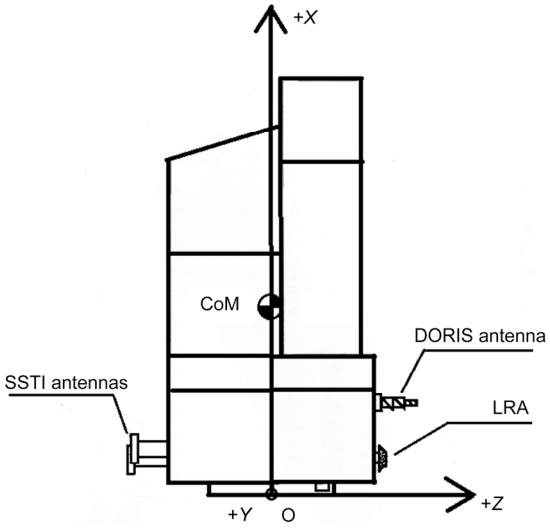

Figure 1 Schematic view on SSTI antennas, LRA, and DORIS antenna on HY2A.

Table 2 Coordinates of HY2A initial CoM and its variation, onboard SSTI-A antenna, DORIS 2 GHz phase center and spherical center of LRA in SRF (unit: mm)

	X_{SRF}	Y_{SRF}	Z_{SRF}
Initial Coordinates of CoM	1246.4	0.0	0.8
CoM variation[a)]	86.0	7.0	8.0
SSTI-A antenna	351.9	−177.9	−1365.4
Spherical center of LRA	311.3	−213.8	994.4
DORIS 2 GHz phase center	850.0	−750.0	1306.0

a) See ftp://ftp.ids-doris.org/pub/ids/satellites/h2amass.txt (accessed on 11 March 2014).

observations indicates that this receiver can provide precise carrier-phase observations with 1–2 mm for L1 and 2–3 mm for L2. We assess the performance of the receiver using GPS data delivered by NSOAS in this contribution. Five types of observations are recorded in the decoded RINEX files with 1 Hz sampling rate: C/A-code (C/A) and P-code measurements (P1 and P2) as well as carrier-phase measurements (L1 and L2).

Figure 2 shows numbers of observations during one typical 30 h POD arc, which is from 21:00 of DOY (Day Of Year) 302/2011 to 3:00 of DOY 304/2011. It can be seen that there are more tracking losses in L2 observations than those in L1 ones. This is probably because of weaker acquisition for L2 measurements during the ascent of GPS satellites. The stronger code correlation acquisition technique makes fewer C/A and L1 observations missed, thanks to that the C/A code structure modulated on L1 phase is open and known. However, P-code and L2 carrier-phase measurements are generated using the so-called Z tracking technique because the P-code structure is unknown. In addition, the transmitted power for L2 phase is designed to be lower than that of L1 one. Consequently, the reception of L2 measurements is slightly worse.

The sky-plot shown in Figure 3 represents the number of L2 losses with elevation and azimuth in antenna reference frame (ARF). The *X*-axis and *Y*-axis of ARF are coincided with that of SRF and point to the same positive directions, and the *Z*-axis completes the left-hand reference frame with pointing to the radial direction. In the ARF, the azimuth is measured from the +*X*-axis, e.g., the direction of satellite flying, to the +*Y*-axis, and the elevation is measured positive towards the zenith (+*Z*-direction). The number of missed observations is obviously elevation dependent and symmetrical distribution in horizontal plane, especially in the regions with azimuth from 240° to 300° and 60° to 120°. There are less than 8% of data affected by the L2 losses and mainly distributed in low elevations, so that the effect on the POD remains limited. This will be demonstrated with POD results in Section 4.

Figure 4 provides percentages of all tracked and useful GPS satellites per epoch (on average) for the aforementioned 30 h POD arc. All tracked and useful satellites are numbered for each epoch, and the percentages of each group (i.e., different satellite numbers) are computed with respect to the numbers of whole tracked and valid satellites, respectively. The histogram shows that the middle number of tracked satellites is seven, whereas it is six for useful satellites. It can be seen that more than 4 satellites are tracked simultaneously in above 98% epochs, and 5 useful satellites are still available for more than 90% epochs after

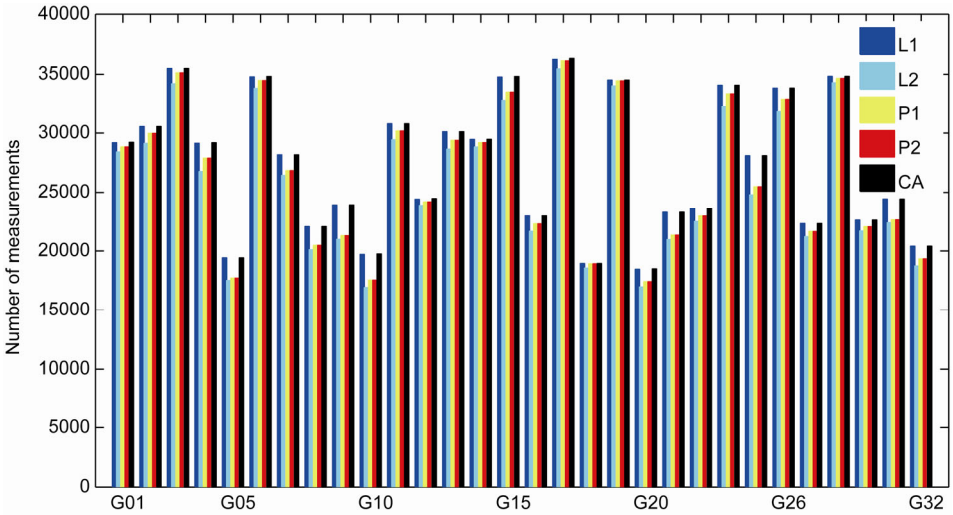

Figure 2 Data availability for five types of observations collected by HY2A onboard GPS receiver: C/A (black), P1 (yellow), and P2 (red) code measurements, as well as L1 (blue) and L2 (cyan) carrier-phase observations for 30 h (no G24 and G27).

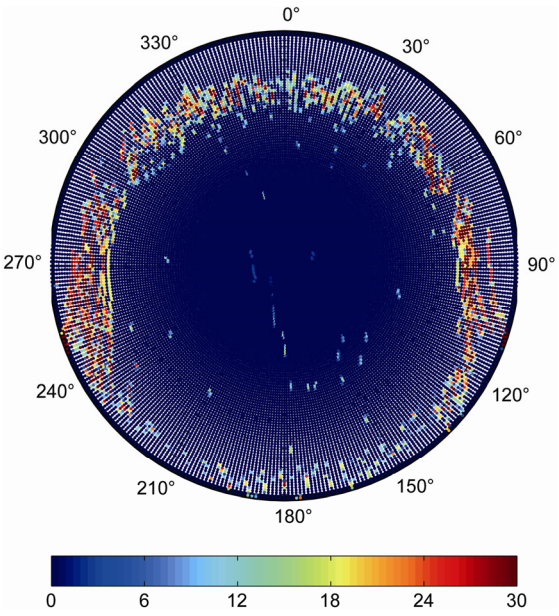

Figure 3 Sky-plot of number of L2 losses for HY2A onboard GPS receiver.

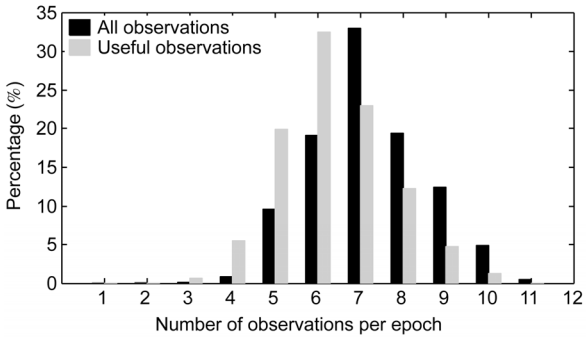

Figure 4 Numbers of all tracked (black) and useful (gray) GPS satellites per epoch.

quality check. These indicate that the ability of simultaneous tracking satellites is strong, and data quality of observations is sufficiently good. In this case, real-time and kinematic POD may be even possible with this type of receiver. This is rather promising for Chinese-own satellite gravimetric projects.

Figure 5 demonstrates the daily ratio of lost epochs to all epochs. In general, GPS observations are available for 239 days and only one day (20 April 2012) has no GPS data for the entire study period. It is noticed that the data used in this contribution were delivered by NSOAS in 2012. The re-delivered data in 2013 appear to have no data gap for 20 April 2012. Furthermore, there are 221 days with the data availability being more than 95%. Fewer data gaps indicate good performance for HY2A onboard GPS receiver, and high accurate orbit solutions are achievable with these data. However, the measurements are rather rare for several days, such as 10 January 2012 (only 48.3% GPS data available). These data gaps may have a negative effect on POD, but

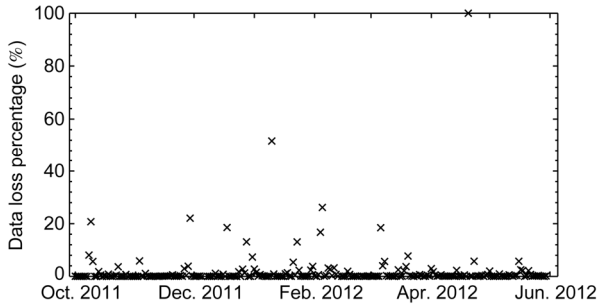

Figure 5 GPS data gap for HY2A from 1 October 2011 to 31 May 2012.

this can be compensated by other tracking systems, e.g., DORIS and SLR. We will show some results in Section 4.

The Multipath Combinations (MPCs) are often used to assess multipath and code noise level of a receiver. The combination is constructed using a single-frequency code measurement and dual-frequency phase measurements of a pass that one receiver is continuously tracking one GPS satellite without cycle slips. The MPCs for HY2A code observations are determined by TEQC (Estey and Meerten, 1999) and the figures are plotted using TEQCSPEC toolkit (Ogaja and Hedfors, 2007).

Figure 6 illustrates the time series of MPCs for HY2A code observations during the period 21 h to 22.5 h of DOY 302/2011. In this figure, the interval between two consecutive PRN numbers along the vertical axis is 1 m, and one color is associated with one individual GPS satellite. The horizontal axis represents time. In general, the MPCs of C/A are larger than that of P1, and that is caused by different accuracy of C/A and P code measurements. The typical noise level of the C/A codes can be 1–3 m, whereas that is about 0.3 m for P codes. A noticeable phenomenon is that the MPCs are rather stable in the middle of per tracking arc, but they can be up to 6 m and vary dramatically during the ascent and descent of GPS satellites. This is obviously caused by the MPCs in low elevations. This is similar to the case of CHAMP and COSMIC satellites with BlckJack receiver, reported by Montenbruck and Kros (2003) and Hwang et al. (2010), respectively.

Figure 7 displays variations of MPCs for C/A- and P-code measurements associated with elevation and azimuth in the sky plot during 21 h of DOY 302/2011 to 3 h of DOY 304/2011. Overall, the multipath effects show different patterns for C/A, P1, and P2 code observations. The large C/A multipath errors, in general, are mainly evenly distributed in low elevation areas (see Figure 7(a)). The multipath effects of P2 are slightly different. Some positive errors are distributed in the fore-looking hemisphere (see Figure 7(c), and notice that different color bar is used). The noise level is smaller than that of C/A. Compared with that of C/A and P2, the P1 MPCs show abnormal pattern: positive values are confined to the aft-looking hemisphere, particularly around the trip of elevation 20°, whereas negative ones are centered mainly on the fore-looking part. This needs further investi-

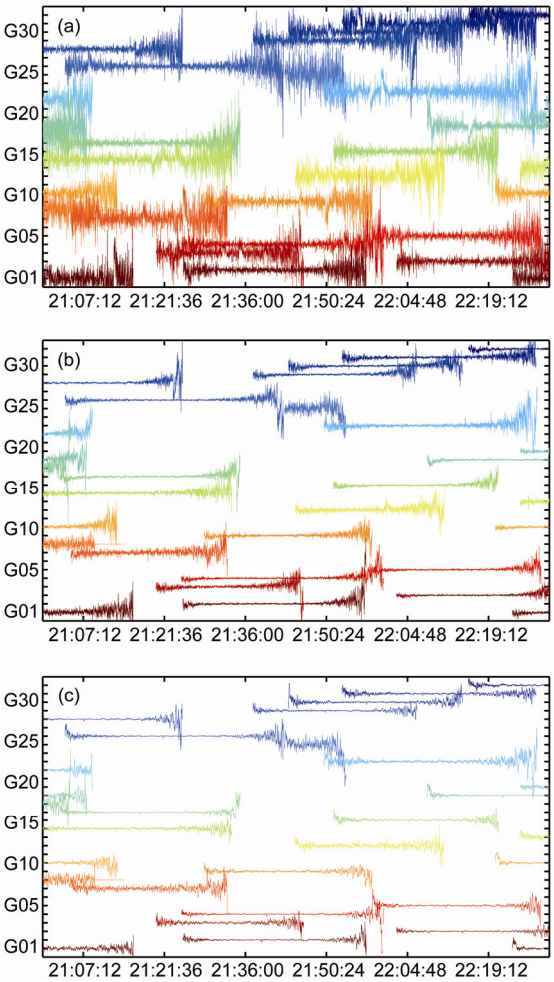

Figure 6 MPCs of C/A (a), P1 (b), and P2 (c) code measurements of HY2A onboard GPS receiver. The interval between two consecutive PRN numbers along the vertical axis is 1 m.

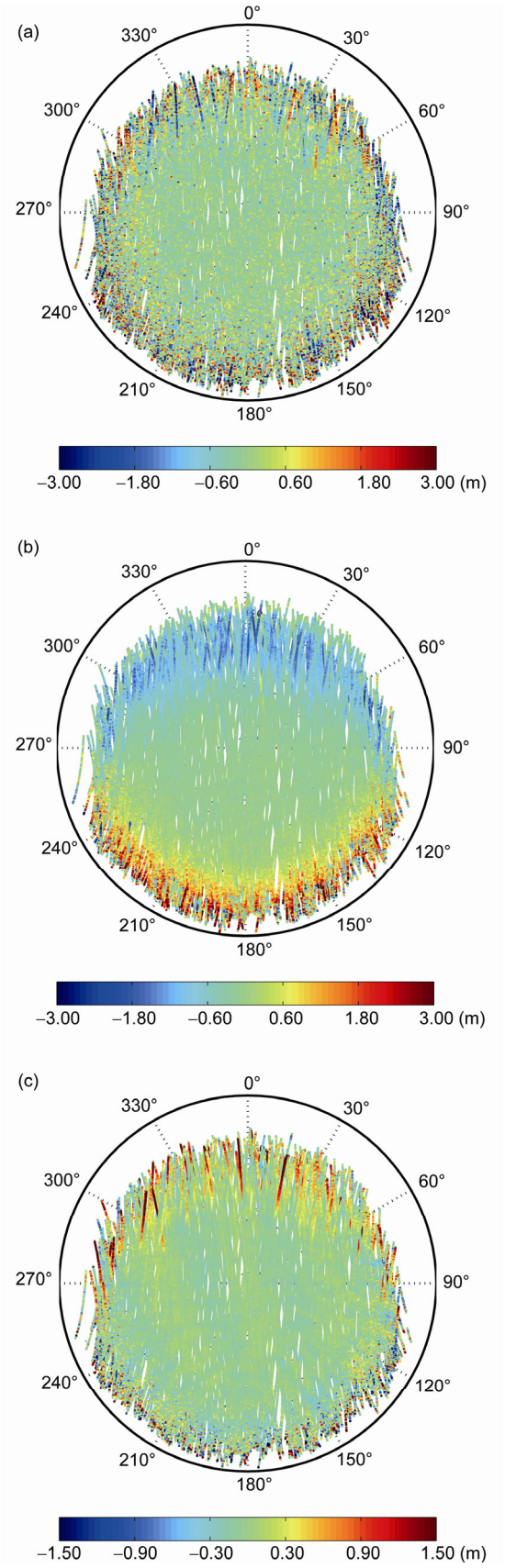

Figure 7 Sky-plots of HY2A MPCs for C/A (a), P1 (b), and P2 (c) code observations.

gation. In general, the averaged RMSs of MPCs for C/A-, P1-, and P2-code measurements are 0.897, 0.385, and 0.320 m, respectively.

The results of only 30 h data are shown in the section as an example, and similar results are obtained for other data arcs as to our analysis up to DOY 147, 2013. Although there are L2 losses and abnormal P1 multipath pattern for HY2A onboard GPS receiver, these code and carrier phase measurements are used to perform POD for the period from 1 October 2011 to 31 May 2012.

2.2 DORIS and SLR tracking data

We use the Doppler observations provided by International DORIS Service (IDS) to perform orbit analyses (Willis et al., 2010). The SLR tracking data delivered by International Laser Ranging Service (ILRS) are used in this study (Pearlman et al., 2002). In Figure 8, we summarize the SLR and DORIS data used for the orbit analyses in this paper. The average numbers of DORIS station passes per day range

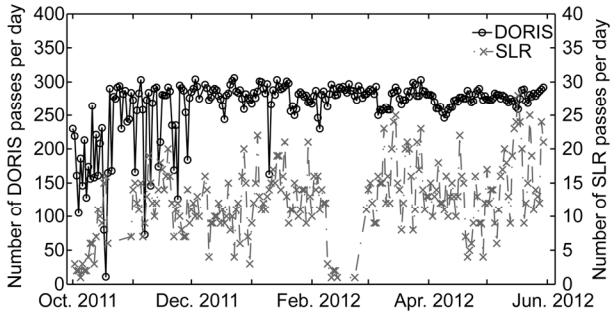

Figure 8 Available DORIS and SLR data for HY2A.

from 250 to 300, slightly more than those of Jason-1 (from 200 to 230) (Lemoine et al., 2010), because seven beacons are simultaneously tracked by the DGXX DORIS receiver equipped by HY2A. However, the DORIS observations at the beginning life of HY2A (October 2011) are rare, and the number of passes is below 200 for most of these days. The situation is likely caused by the lack of frequency estimation due to a huge maneuver (Dejus et al., 2012). After December 2011, the number of passes per day is rather stable, which indicates that the instrument is in good condition. The ILRS network stations have supplied between 10 and 20 SLR passes per day on average. The similar results have been shown in figure 3 of Zhao et al. (2012). Although the tracking priority of HY2A is not higher than that of Jason series satellites for the ILRS network, the number of passes per day increases gradually, resulting in sufficient observations available for this study.

The ILRS network is not well distributed over the northern and southern as well as the eastern and western hemispheres (Pearlman et al., 2002; Zhao et al., 2012). A subset of the ILRS stations supplies the bulk of the SLR tracking, whereas others provide only a few (see Figure 9). The SLR stations providing most of data for HY2A are Yarragadee, Australia (Monument ID: 7090); Changchun, China (Monument ID: 7237); Greenbelt, Maryland, US (Monument ID: 7105); Zimmerwald, Switzerland (Monument ID: 7810). Particularly, Yarragadee provided more than 600 passes during the selected period, more than twice of that provided by Changchun. Similar result has been shown in Zhao et al. (2012), but the number and the statistics are slightly different due to different analysis period used.

In addition, Figure 10 shows the HY2A DORIS stations visibilities with 5° elevation mask. It can be seen that there are still areas where ground tracks are not available for HY2A, though the DORIS track network consists of 58 beacons that are reasonably well distributed at this stage.

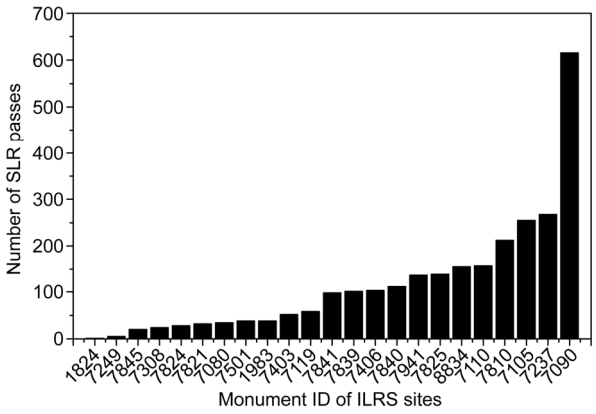

Figure 9 Number of SLR passes provided by ILRS sites for HY2A during the selected study period.

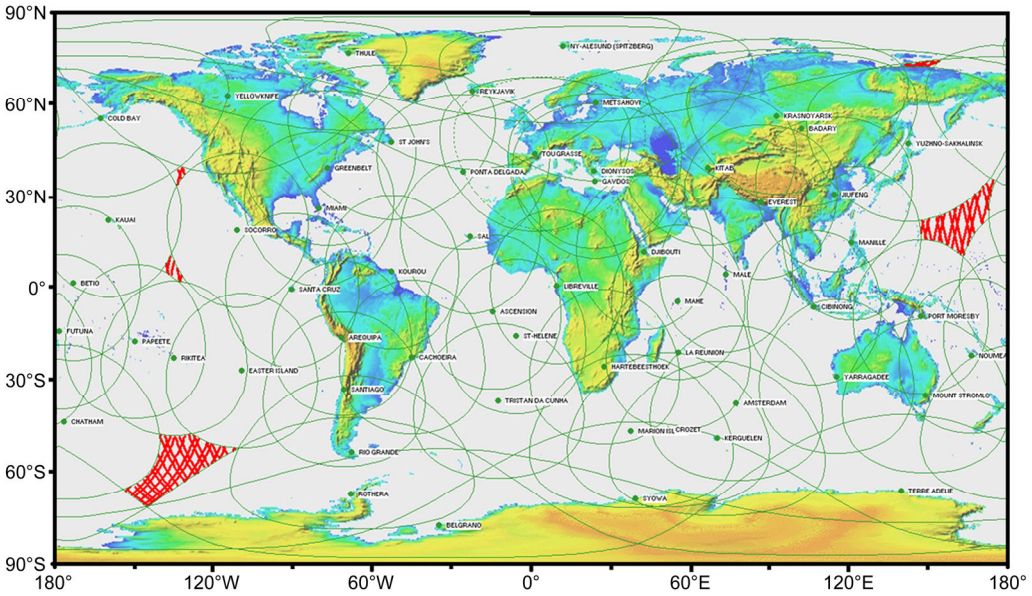

Figure 10 HY2A DORIS stations visibilities with 5° elevation mask (from http://ids-doris.org/images/doris/HY-2A-NonCoveredGroundTrack. png). The areas with red lines are visibility holes.

Although these areas with visibility holes are located mainly in the Pacific Ocean and the regions near the Antarctic, the DORIS orbit solutions should not be significantly affected by these holes.

3 POD strategy and solutions validation

3.1 Dynamic or reduced-dynamic orbit determination

The dynamic orbit determination is based mainly on the description of the gravitational and non-gravitational forces in the equations of motion. The orbit is computed arc-by-arc. The satellite initial state of each arc and a limited set of piece-wise empirical parameters are estimated using observations. The gravitational and non-gravitational forces are used to accurately transit the initial state vector to the orbit of the whole arc. The purely dynamic POD results in robust continuous positions even within data gaps, but the dynamic orbit accuracy relies heavily on the accuracy of force models. The force model errors result in systematic orbit errors growing with the arc length. In order to reduce the orbit errors, the reduced-dynamic orbit determination technique is proposed (Yunck et al., 1994; Bertiger et al., 1994). The reduced-dynamic orbit determination introduces an additional number of stochastic accelerations or pulses to attenuate the unmodeled or mismodeled force model errors. However, the reduced-dynamic solutions need denser and geometrically stronger tracking data. Therefore, the reduced dynamic orbits are less sensitive to dynamic modeling errors, but more to measurement errors. The force models are significantly improved in last couple of years since the GRACE and GOCE gravity missions were successfully used to determine static/temporal gravity filed models (Förste et al., 2011). However, considering data gaps, we prefer dynamic, rather than reduced-dynamic, orbit determinations for HY2A POD, in order to limit the dependency of the orbit accuracy on gaps in the measurements (see last section), especially for DORIS and SLR data processing.

3.2 Models and parameters used for orbit determination

Precise force models are key elements for dynamic orbit determination. Both static and temporal force models must be considered for LEOs, such as HY2A. A series of precise static gravity field models have been developed and improved dramatically compared to JGM used for T/P POD (Hashemi-Farahani et al., 2013; Förste et al., 2011; Nikolaos et al., 2012). In addition, the variability in Earth gravity field has an impact on orbit solutions for LEOs and should be modeled in the POD strategy. For example, Zelensky et al. (2010) shows that the time-variable gravity induces a geographically coherent annual signal in the radial component of the Jason-1 orbits with amplitude of 5 mm. The newly released EIGEN-6C is produced from the combination of LAGEOS, GRACE, GOCE, and DTU10 global gravity anomaly data (Förste et al., 2011). Besides the static part with maximum degree and order of spherical harmonic coefficients up to 1420, this model also contains time variable parameters up to degree and order 50. EIGEN-6C is used here to model both static and temporal gravity signals. The GRACE atmosphere and ocean de-aliasing products are used for modeling atmosphere pressure and ocean bottom mass variations. The latest ocean tide model (Lyard et al., 2006) and ocean pole tide (Desai, 2002) are used as well.

Another error source of POD is surface force mis-modeling. The non-conservative forces acting on the satellite surface are due primarily to SRP and atmospheric drag. However, the effects of solar radiation at the HY2A altitude of 970 km are typically larger than effects of air drag. The difficulty in modeling effects of radiation forces is due largely to the complex satellite geometry and incomplete knowledge of the reflective, as well as thermal properties of satellite surfaces. A box-wing model has been developed to compute the SRP from a set of flat plates of known optical properties, areas, and surface orientation (Marshall and Luthcke, 1994). Actually, the box-wing model is only as a means to compute the complete radiation force and not as an actual box with meaningful physical properties. A new approach in modeling the radiation forces acting on the satellite is developed by the UCL (Ziebart 2004). Zelensky et al. (2010) shows improvements in SLR residuals are seen over all beta-prime angles for both Jason-1 and Jason-2 using the UCL model. But unfortunately, we have to use the box-wing model for SPR due to currently nonexistence UCL model for the HY2A mission. Table 3 summarizes the force models and data used as well as parameters to be estimated in POD of HY2A. It is noticed that the force models used are different from those in Guo J et al. (2013).

3.3 Data weights for different data types

When different data types are used to perform POD for HY2A mission, it is important to find the optimal relative weights for each measurement type. It seems that the simplest way is to set the weights according to RMSs of post-fit residuals of different data types. However, this is not the case for HY2A POD, because the solutions are affected not only by measurement noise but also by other factors, such as geometrical distribution of observations. Trying to determine the relative weight by variance and covariance estimation is not a trivial matter to obtain optimal solutions either, due to the different density, geometry, and time resolution for each measurement types. Hence, a "leave-one-out" approach was used to find the appropriate weights, and the SLR validation was used as the criterion to determinate the best candidate. First, we determined the orbits using SLR and DORIS data separately, and then computed RMSs of post-fit residuals, which are about 2 cm for SLR and 0.45 mm s^{-1} for DORIS. This is served as the reference for prior standard deviations (i.e., sigma) of each type of data. Second,

Table 3 The summary of POD strategy for HY2A satellite

Analysis strategy	Description
Geophysical models	
Static	Static part of EIGEN-6C up to degree and order 150 (Förste et al., 2011)
Temporal	Temporal part of EIGEN-6C up to degree and order 50 (Förste et al., 2011)
Secular rates for low degree coefficients	IERS Conventions 2003 (McCarthy and Petit, 2004)
n-body	JPL DE405
Solid earth tides	IERS Conventions 2003 (McCarthy and Petit, 2004)
Ocean tides	FES2004 (Lyard et al., 2006)
Atmosphere and ocean de-aliasing	AODL1B RL05 (Flechtner, 2007)
Ocean pole tides	Desai (2002)
Relativistic effects	IERS Conventions 2003 (McCarthy and Petit, 2004)
Satellite surface models and attitude	
Atmospheric drag	DTM94 (Berger et al., 1998)
Solar radiation pressure	Box-wing
Attitude	Nominal
Reference frame	
Inertial frame	J2000.0
SLR	ITRF2008-TRF-ILRS (Atamimi et al., 2011)
DORIS	DPOD2008 (Willis et al., 2011)
Earth tide and ocean loading	IERS 2003 (McCarthy and Petit, 2004)
Precession/nutation	IAU 2000A
EOP	IERS EOP 08 C04 (IAU2000A)
Tracking data	
GPS	Undifferenced ionosphere-free phase and code (interval 30 s)
DORIS	IDS DORIS 2.2 format
SLR	ILRS CRD
GPS orbits	IGS final orbits
GPS clock	IGS 30 s final clock products
GPS antenna phase center correction	IGS08 (Schmid, 2011)
HY2A PCO and PCV	Calibrations in orbit
Weight	
GPS, GPS+DORIS, GPS+DORIS+SLR	3 cm for GPS phase and 6 m for code measurements
	1 mm s^{-1} for DORIS
	10 cm for SLR
DORIS, DORIS+SLR	1 mm s^{-1} for DORIS
	10 cm for SLR
Measurement parameters	
GPS	Real constant value for each ambiguity pass
	Epoch-wise receiver clock offset
DORIS	Constant bias for each pass
Dynamical parameters	
GPS, GPS+DORIS, GPS+DORIS+SLR	Drag coefficient every 300 min
	Empirical coefficients in along- and cross-tracking every 600 min
DORIS, DORIS+SLR	Drag coefficient every 900 min
	Empirical coefficients in along- and cross-tracking every 900 min
POD arc length	30 h

we combined SLR and DORIS data to perform POD, and the sigmas were adjusted to determine the best orbit solution validated by SLR. After intensive trials, the sigmas for SLR and DORIS were set as 10 cm and 1 mm s^{-1} respectively, which are larger than the RMSs of the post-fit residuals (e.g., the reference value). Afterward, the GPS observations were added to perform POD with SLR and DORIS data together. In this case, the sigma values for SLR and DORIS were fixed as the aforementioned values, but only the prior sigmas for GPS code and phase observations were tuned. Finally, we fixed the prior sigmas as 3 cm and 6 m for GPS phase and code observations respectively after intensive trials. Because we have found that the GPS data would suppress the SLR and DORIS data if a higher weight for GPS phase observations was set, whereas a lower weight could have made the solutions contaminated by DORIS and

SLR. It is noticed that the weights we use in this study may be not the optimal one, and this is still open to further investigation.

Regarding the elevation mask for each type of measurements, we do not set the limited value for any type observations but only down-weight those measurements with low elevations. It is noticed that the DORIS data delivered by IDS have been edited on the basis of the elevation mask being set as degree 10.

3.4 GPS antenna phase center modeling

Proper modeling of the GPS receiver instantaneous antenna phase center is important to the overall performance of the GPS-based solutions. Prior to the launch of T/P, it was recognized that phase center variations of the onboard antenna were significant, and should be measured and modeled. Early efforts to apply phase center models were only partially successful (e.g., Bertiger et al., 1994), because antenna phase variations of the GPS transmitters were not accounted for. With the development of competing models for the GPS transmitter PCV based on terrestrial data (Schmid et al., 2005), the PCV of onboard GPS receiver antenna became an important error, which should be modeled, in order to achieve 1 cm radial RMS accuracy for altimetry and other LEO satellites. Measurements of the PCO and PCV taken prior to the launch do not reflect actual space environment once the antenna is mounted on the spacecraft. Therefore, further calibration and modeling are necessary. The unmodeled or mismodeled PCV may be partially absorbed by post-fit residuals. Luthcke et al. (2003) and Haines et al. (2004) used post-fit phase residuals to develop an empirical PCV map for Jason-1. Furthermore, Jäggi et al. (2009) also calibrated phase center variations for GRACE mission by both residual approach and direct approach.

Although the empirical PCO and PCV of HY2A GPS receiver antenna were provided prior to launch, the initial analysis of the GPS data indicated that there was a significant system error of residuals in the zenith, attributable to improper phase variations (Guo J et al., 2013). Hence, we re-calibrated the PCO and PCV for HY2A onboard GPS receiver antenna. The solution was determined using data from 30 h arcs obtained from 1 October 2011 to 31 May 2012.

For the PCO calibration of the onboard GPS receiver antenna, Choi (2003) demonstrates in the Jason-1 case that the *X*-component of PCO could only be estimated when the *X*-axis of ARF is perpendicular to the direction of satellite velocity due to high correlation between *X*-component of PCO and along-tracking empirical parameters. The *Y*-component PCO could not be separated with other orbit parameters. Therefore, it is difficult to estimate the *X*- and *Y*-component of PCO. The *Z*-component could only be determined if there is no empirical constant acceleration in radial. The *Z*-component PCO, compared with other two, plays a significant role in improvement of orbit solutions. HY2A orbits the Earth in a sun-synchronous orbit, so the elevation of sun with respect to the orbit plane is almost constant and the attitude control is simple and stable. Under the nominal attitude and POD strategy, only the *Z*-component parameter of PCO for each orbit arc was estimated simultaneously with those orbit parameters. Figure 11 shows the estimated values during the study period. A dramatically leap up to −1.2 cm can be seen on 10 October 2011. This is also likely due to a significant orbit maneuver in the beginning of the life time of HY2A. During this period, the fuel consumption resulted in the CoM drift.

As far as the PCV calibration is concerned, we use post-fit residuals of GPS ionosphere-free phase measurements to estimate the PCVs under the assumption that the unmodeled PCV errors could be absorbed by residuals. The PCVs are modeled as grid with 5°×2° resolution in azimuth and elevation (see Figure 12). There are 3241 parameters to be estimated, which represent the PCVs in specific grid points. However, those parameters in low elevations should be highly constrained due to data gap caused by the L2 losses (see Figure 3) and data quality check, and for detailed information, please refer to Guo J et al. (2013).

Table 4 summarizes the performance of HY2A solutions with PCO and/or PCV corrections compared with those solutions without using PCO and PCV at all. In the case that both PCO and PCV are not used, the post-fit residuals of GPS ionosphere-free phase measurements are at the level of 13.6 mm, RMS for SLR validation is 17.5 mm, and the radial orbit difference with respect to the CNES precise orbit ephemerides (POEs) is 7.2 mm. The solution with PCO only corrections shows a dramatic improvement. The RMSs of GPS phase post-fit residuals and radial orbit differences reduce to 8.5 and 6.2 mm respectively, whereas the SLR validation improve about 9.1% (from 17.5 to 15.9 mm). The improvements on the SLR validation and radial differences are no longer significant when PCV corrections are added, but the RMS of post-fit residuals reduces by 1 to 7.5 mm. In conclusion, the phase center offset calibration is essential for high accuracy POD. The orbit accuracy shown in Table 4 shows dramatic improvements compared with that in Guo

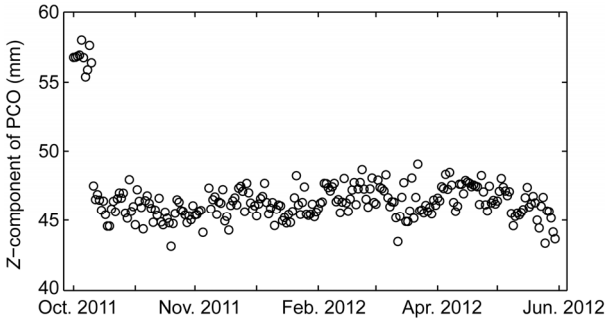

Figure 11 Estimated *Z*-component PCO for HY2A onboard GPS antenna in ARF.

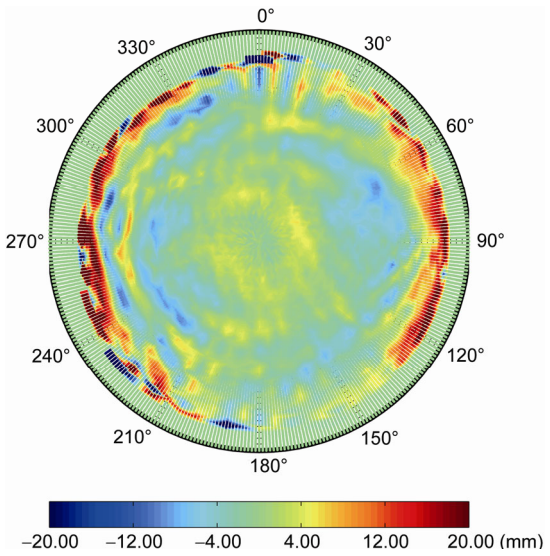

Figure 12 Azimuth-elevation diagram of the 5°×2° PCVs (mm) for the ionosphere-free linear combination of the HY2A onboard GPS receiver antenna.

J et al. (2013) (see Tables 3 and 4 of that publication), thanks to that better force models and refined data processing strategies used in this contribution.

3.5 Orbit validation

We have computed six sets of precise orbits using different combinations of GPS, DORIS, and SLR tracking data for the period from 1 October 2011 to 31 May 2012. For solutions produced using GPS data, the calibrated PCVs are used to eliminate phase variation errors, and the PCOs are estimated with orbit parameters. The easiest way to evaluate the consistency of satellite orbits is to directly compare positions from different orbit solutions. For example, we compare our solutions with the external CNES POEs determined using a combination of GPS, DORIS, and SLR data as well. The CNES POEs solutions are considered as the best ones obtained so far. Furthermore, we determine the orbit with 30 h arc for each set of solutions, so that there is an overlap of six hours between two adjacent orbits, which can be used for internal orbit validation for each individual set of solution. Finally, the SLR Observed minus Computed (O-C) residuals are used to validate the accuracy of orbit solutions (no mask elevation is set for SLR validation). However, the accuracy of altimeter measurements is about 8.0 cm (Zhang et al., 2013), much lower than the orbit accuracy; therefore, the altimeter data are not used to validate the orbit.

Table 5 presents the statistic results for orbit differences and SLR O-C residuals of the whole period for dependent and independent comparisons. Let us first discuss those solutions without using GPS data. It can be seen that the DORIS only solutions already provide centimeter accuracy. The DORIS+SLR solutions are slightly better than the DORIS only solutions on orbit differences if the CNES POEs are taken as reference. The radial component and 3D differences reduce by 0.8 and 3.4 mm, respectively. However, the orbit overlapping comparison becomes slightly worse. The orbit differences between these two types of solutions (DORIS+SLR and SLR) are 1.2 mm for the radial component and 10.0 mm for three components. Hence, it can be concluded that the DORIS+SLR solutions relied more heavily on the DORIS data. This is because the DORIS data have better temporal and spatial coverage than SLR tracking observations.

In addition, the solutions using GPS tracking data combined with/without other types of measurements show almost the same performance on orbit differences, overlap differences, and SLR fits. Variations of different solutions on orbit differences with respect to the CNES POEs are only 0.1 mm in the radial component and 0.3 mm in three components. Meanwhile, variations of overlap differences are also rather small (about 1.0 mm). All of these indicate that the HY2A solutions rely heavily on GPS data because GPS tracking data have denser and more evenly geometrical distribution. However, it does not mean that the combination of multi-type measurements makes no contribution to accuracy of solutions. As can be seen from Table 5, the GPS combined solutions with DORIS data show improvement in orbit overlapping comparison with respect to that without DORIS. Furthermore, the SLR validation can be improved by adding the SLR data. Although GPS+SLR solutions are not independent of SLR data, we do observe a slight improvement in SLR fits over any other solutions. Furthermore, the combination of multi-type observations could attenuate orbit errors caused by data gaps. Figure 13 shows daily 3D RMSs of orbit differences between GPS only as well as GPS+DORIS+SLR combined solutions with respect to CNES POEs, respectively. It can be seen that the RMS value of orbit differences can be up to above 60 mm on 10 January 2012 when only 48.3% GPS data are available,

Table 4 Solution comparison with/without PCO and/or PCV calibration[a)]

Solutions	Orbit differences with respect to CNES POEs (mm)				Residuals (mm)	SLR (mm)	
	A	C	R	3D		Mean	RMS
Without PCO & PCV	28.2	20.9	7.2	35.8	13.6	–0.3	17.5
PCO only	21.8	19.7	6.2	30.1	8.5	0.6	15.9
With PCO & PCV	22.2	19.7	6.1	30.3	7.5	0.1	15.6

a) GPS measurements are only used for orbit determination. A: Along-track; C: Cross-track; R: Radial.

Table 5 Statistics of HY2A orbit differences with respect to the CNES POEs, statistics of 6 h overlap differences, and statistics of SLR fit [a)]

Solutions	Orbit differences with respect to CNES POEs (mm)		Overlap differences (mm)		SLR O-C (mm)	
	Radial (RMS)	3D (RMS)	Radial (RMS)	3D (RMS)	Mean	RMS
DORIS	10.0	52.7	7.5	43.3	0.9	27.8
DORIS+SLR	9.2	49.3	8.0	47.3	0.6	18.4
GPS [b)]	6.3	32.6	5.5	20.6	0.5	17.5
GPS+DORIS	6.4	32.5	5.3	19.8	0.4	17.6
GPS+SLR	6.3	32.4	5.5	20.2	0.3	16.6
GPS+DORIS+SLR	6.3	32.3	5.3	19.5	0.3	16.9

a) These orbit solutions are produced with different data combinations; b) The differences w.r.t. solution with PCV and PCO in Table 4 is caused by different days used for statistic, because some days are excluded due to DORIS or SLR data unavailable, although the GPS solutions are available.

and it is reduced significantly to 47 mm if combined with other tracking measurements.

As a whole, statistics of orbit overlapping differences, SLR O-C residuals, and cross-comparison of CNES POEs obtained with different tracking techniques indicate that the radial accuracy of our orbits is at the 1.0 cm level for HY2A mission. Specifically, the average daily RMSs of the radial differences between our orbits and CNES POEs are below 7 mm.

4 Conclusions

In this paper, we assess the performance of onboard GPS receiver carried by the HY2A satellite. The receiver performs well despite about 8% unexpected L2 tracking losses in low elevation, particularly during the ascent of GPS satellites. This is due mainly to the weak acquisition for L2 observations. However, the effect of these losses on the POD remains limited. Analysis of the number of all tracked and useful satellites shows that more than four satellites are tracked in more than 98% epochs and five useful satellites are still available for 90% epochs after data editing.

For multipath error analyses, those multipath effects show different patterns for C/A, P1, and P2 code measurements. The larger C/A multipath errors are evenly distributed mainly in low elevation areas, whereas the multipath effects of P2 are somehow different. The level is smaller than that of C/A and some positive errors are located in the fore-looking hemisphere. Multipath errors of P1 show an abnormal pattern, and positive errors are confined to the aft-looking hemisphere, particularly around the trip of elevation 20°. However, negative errors are distributed on the fore-looking part. This needs further investigation.

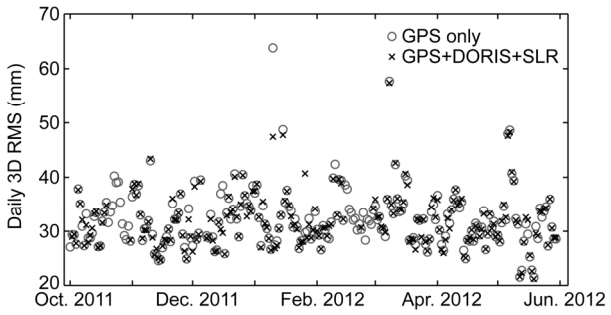

Figure 13 Daily 3D RMSs of orbit differences of GPS only (gray) and GPS+DORS+SLR (black) solutions with respect to the CNES POEs. If any type of data is missing, the combined solution is not determined.

Proper modeling of the GPS receiver instantaneous antenna phase center is important to the overall performance of the GPS-based solutions to achieve 1.0 cm accuracy. In this paper, we also modeled the PCO and PCV for HY2A onboard GPS receiver antenna. A significant jump for *Z*-component of PCO up to −1.2 cm exists on DOY 283/2011. It is likely caused by huge orbit maneuver. With PCO and PCV maps for GPS only solutions, post-fit residuals reduce to 7.5 mm, and radial orbit differences with respect to CNES POEs improve to 6.1 mm. Meanwhile, SLR fits improve about 9.1% (from 17.5 to 15.9 mm).

Statistics of SLR residuals and cross-comparison of our orbits and CNES POEs indicate that the accuracy of radial orbits is at the 1.0 cm level for HY2A solutions. Orbits computed using GPS tracking data with or without combination of other types of measurements show almost the same performance on orbit differences, overlap differences, and SLR fits. That indicates the HY2A solutions rely heavily on GPS data. However, the combination of multi-type observations not only can improve the accuracy slightly, but also can attenuate the orbit errors caused by data gaps. This is particularly important for some occasional periods when the GPS receiver performs badly.

The result obtained in the contribution is a preliminary achievement for HY2A orbit determination. However, it demonstrates that the Chinese indigenous GPS receiver can be used to determine precise orbits for LEOs with rather high accuracy. In this paper, the followings are not covered but need further investigation. It is possible to fix GPS ambiguities into their integers if uncalibrated phase delays are computed and applied. Solutions may be improved further. Phase and code observations of DORIS can be directly processed with epoch differenced or un-differenced approach, instead of Doppler observations. The 8-day orbit arcs for HY2A are probably used to replace the current 30 h ones. The last but not the least, a detailed analysis for radial error budget still needs further investigations. Understanding

their contributions to the radial errors is essential for further improvements of the orbit accuracy.

This work was supported by the National Natural Science Foundation of China (Grant No. 41231174), the Open Fund of Key Laboratory of Precision Navigation and Technology, National Time Service Center (Grant No. 2012PNT06), and the Fundamental Research Funds for the Central Universities of China (Grand No. 2012618020201). The GPS, DORIS, and SLR tracking data are provided by NSOAS, IDS, and ILRS respectively. The CNES POEs are delivered by IDS. Finally, we thank the anonymous reviewers for their constructive remarks that help improve the quality of the manuscript.

Atamimi Z, Collilieux X, Métivier L. 2011. ITRF2008: An improved solution of the international Terrestrial Reference Frame. J Geodesy, 85: 457–473

Auriol A, Tourain C. 2010. DORIS system: The new age. Adv Space Res, 46: 1484–1496

Berger C, Biancale R, Barlier F, et al. 1998. Improvement of the empirical thermospheric model DTM: DTM94—A comparative review of various temporal variations and prospects in space geodesy applications. J Geodesy, 72: 161–178

Bertiger W I, Bar-Sever Y E, Christensen E J, et al. 1994. GPS precise tracking of TOPEX/POSEIDON: Results and implications. J Geophys Res-Oceans, 99: 24449–24464

Bertiger W, Desai S D, Dorsey A, et al. 2010. Sub-centimeter precise orbit determination with GPS for ocean altimetry. Mar Geodesy, 33: 363–378

Cerri L, Berthias J P, Bertiger W I, et al. 2010. Precise orbit determination standards for the Jason series of altimeter missions. Mar Geodesy, 33: 378–418

Choi K R. 2003. Jason-1 precision orbit determination using GPS combined with SLR and DORIS tracking data. Doctoral Dissertation. Austin: The University of Texas at Austin

Dejus M, Auriol A, Mercier F, et al. 2012. DORIS on HY-2A. IDS Workshop, Venice, Italy

Desai S D. 2002. Observing the pole tide with satellite altimetry. J Geophys Res-Oceans, 107: 3186–3198

Estey L H, Meerten C M. 1999. TEQC: The multi-purpose toolkit for GPS/GLONASS data. GPS Solut, 3: 42–49

Flechtner F. 2007. AOD1B Product Description Document. GRACE project document 327–750, Revision 3.1

Förste C, Bruinsma S, Shako R, et al. 2011. EIGEN-6—A new combined global gravity field model including GOCE data from the collaboration of GFZ-Potsdam and GRGS-Toulouse. EGU General Assembly 2011, Vienna, Austria

Fu L L, Christensen E J, Yamaron C A, et al. 1994. TOPEX mission overview. J Geophys Res-Oceans, 99: 24369–24381

Guo J, Zhao Q L, Li M, et al. 2013. GPS-derived cm level orbit for HaiYang 2A satellite (in Chinese). Geomat Inf Sci Wuhan Univ, 38: 52–55

Guo J Y, Kong Q L, Qin J, et al. 2013. On precise orbit determination of HY-2 with space geodetic techniques. Acta Geophys, 61: 752–772

Guo J Y, Qin J, Kong Q L, et al. 2012. On simulation of precise orbit determination of HY-2 with centimeter precision based on satellite-borne GPS technique. Appl Geophys, 9: 95–107

Haines B, Bar-Sever Y, Bertiger W, et al. 2004. One-centimeter orbit determination for JASON-1: New GPS-based strategies. Mar Geodesy, 17: 299–318

Hashemi Farahani H, Ditmar P, Klees R, et al. 2013. The static gravity model DGM-1S from GRACE and GOCE data: Computation, validation and an analysis of GOCE mission's added value. J Geodesy, 87: 843–867

Hwang C, Tseng T P, Lin T J, et al. 2010. Quality assessment of FORMOSAT-3/COSMIC and GRACE GPS observables: Analysis of multipath, ionospheric delay and phase residual in orbit determination. GPS Solut, 14: 121–131

Jäggi A, Dach R, Montenbruck O, et al. 2009. Phase center modeling for LEO GPS receiver antennas and its impact on precise orbit determination. J Geodesy, 83: 1145–1162

Jiang X, Wang X, Peng H, et al. 2013. The technology of precise orbit determination for HY-2A satellite (in Chinese). Engineering Sci, 15: 19–24

Lemoine J M, Capdeville H. 2006. A corrective model for Jason-1 DORIS Doppler data in relation to the South Atlantic Anomaly. J Geodesy, 80: 507–523

Lemoine J M, Bruinsma S, Loyer S, et al. 2007. Temporal gravity field models inferred from GRACE data. Adv Space Res, 39: 1620–1629

Lemoine F G, Zelensky N P, Chinn D S, et al. 2010. Towards development of a consistent orbit series for TOPEX, Jason-1, and Jason-2. Adv Space Res, 46: 1513–1540

Luthcke S B, Zelensky N P, Rowlands D D, et al. 2003. The 1-Centimeter Orbit: Jason-1 precision orbit determination using GPS, SLR, DORIS and altimeter data. Mar Geodesy, 26: 399–421

Lyard F, Lefevre F, Letellier T, et al. 2006. Modelling the global ocean tides: Modern insights from FES2004. Ocean Dyn, 56: 394–415

McCarthy D D, Petit G. 2004. IERS Conventions (2003). IERS Technical Note No. 32. IERS Conventions Centre

Marshall J A, Luthcke S B. 1994. Modeling radiation forces acting on TOPEX/POSEIDON for precision orbit determination. J Spacecraft Rockets, 31: 99–105

Montenbruck O, Kroes R. 2003. In-flight performance analysis of the CHAMP BlackJack GPS Receiver. GPS Solut, 7: 74–86

Ogaja C, Hedfors J. 2007. TEQC multipath metrics in MATLAB. GPS Solut, 11: 215–222

Pavlis N K, Holmes S A, Kenyon S C, et al. 2012. The development and evaluation of the Earth Gravitational Model 2008 (EGM2008). J Geophys Res Sol Earth, 117: B04406

Pearlman M R, Degnan J J, Bosworth J M. 2000. The International Laser Ranging Service. Adv Space Res, 30: 135–143

Schmid R, Rothacher M, Thaller D, et al. 2005. Absolute phase center corrections of satellite and receiver antennas: Impact on global GPS solutions and estimation of azimuthal phase center variations of the satellite antenna. GPS Solut, 9: 283–293

Schmid R. 2011. Upcoming switch to IGS08/igs08.atx—Details on igs08.atx. IGSMAIL-6355, available on http://igs.org/pipermail/igsmail/2011/006347.html

Tapley B D, Ries J C, Davis G W, et al. 1994. Precise orbit determination for TOPEX/POSEIDON. J Geophys Res-Oceans, 99: 24383–24404

Willis P, Fagard H, Ferrage P, et al. 2010. The international DORIS service, toward maturity, in DORIS: Scientific application in geodesy and geodynamics. Adv Space Res, 45: 1408–1420

Willis P, Argus D, Cerri L, et al. 2011. DPOD2008: A DORIS terrestrial reference frame for precise orbit determination. OSTST Meeting, San Diego, USA

Wu B. 2012. ILRS SLR mission support request form retroreflector information for HY2A. Available on http://ilrs.gsfc.nasa.gov/docs/HY2_retroreflector.pdf

Yunck T P, Bertiger W I, Wu S C, et al. 1994. First assessment of GPS-based reduced dynamic orbit determination on TOPEX/Poseidon. Geophys Res Lett, 21: 541–544

Zelensky N P, Lemoine F G, Ziebart M, et al. 2010. DORIS/SLR POD modeling improvements for Jason-1 and Jason-2. Adv Space Res, 46: 1541–1558

Zhao G, Zhou X H, Wu B. 2012. Precise orbit determination of Haiyang-2 using satellite laser ranging. Chin Sci Bull, 58: 589–597

Zhang Q, Zhang J, Zhang H, et al. 2013. The study of HY-2A satellite engineering development and in-orbit movement (in Chinese). Engineering Sci, 15: 12–18

Ziebart M. 2004. Generalized analytical solar radiation pressure modeling algorithm for spacecraft of complex shape. J Spacecraft Rockets, 41: 840–849